X Encontro Brasileiro sobre Adsorção
27 a 30 de Abril de 2014
Guarujá - SP

CO_2 ADSORPTION ON AMINE MODIFIED MESOPOROUS SILICAS: STUDY OF THE PROGRESSIVE DISORDER ON THE HONEYCOMB ARRANGEMENT.

E. Vilarrasa-Garcia[1], E.M. Ortigosa Moya[1], J.A.Cecilia[1], C.L. Cavalcante Jr[2]., J.Jiménez-Jiménez[1], D.C.S. Azevedo[2], E. Rodríguez-Castellón[1].

1-Departamento de Química Inorgánica –Facultad de Ciencias- Universidad de Málaga
CP: 29071 – Málaga – Spain
Telefone: (34) 952131873 – Fax: (34) 952131870– Email: castellon@uma.es
2- Department of Chemical Engineering-Universidade Federal do Ceará- Campus do Pici, bl:709.-60455-760-Fortaleza-Brazil

RESUMO: Neste trabalho, estudou-se a influência de alterações na estrutura porosa tipo "favo de mel" típica da classe de sílicas mesoporosas SBA-15 sobre a adsorção de CO_2. SBA-15 foi sintetizada por via hidrotérmica (S00) e por outras rotas que introduziram modificações, como expandir o poro usando heptano (S10), reduzir o comprimento dos canais e modificar a estrutura hexagonal da sílica por adição de quantidades crescentes de fluoreto de amônio (S11, S12, S13 e S14). Todos estes materiais foram funcionalizados pela ancoragem de amino-propil tri-etoxisilano (APTES) à superfície da sílica ou por impregnação de polietilenoimina (PEI). As isotermas de CO_2 foram obtidas e matematicamente tratadas para todos os adsorventes usando o modelo de Langmuir de duplo sítio ("Dual Site") e a influência da estrutura foi relacionada com as diferentes capacidades de CO_2. Comprovou-se que a adição de fluoreto é importante na regulação da quantidade de CO_2 adsorvida por fisissorção e quimisorção.

PALAVRAS-CHAVE: APTES, quimisorçao, fluoreto, SBA-15.

ABSTRACT: In this work, the influence of changes in the typical honeycomb structure of APTES grafted SBA-15 on the adsorption of CO_2 was studied. SBA-15 was synthesized hydrothermally (S00) and by introducing some modifications, such as pore expansion using heptane (S10) and changes in the hexagonal arrangement of the silica by adding increasing amounts of ammonium fluoride (S11, S12, S13 and S14). All of the synthesized silicas had either its surface grafted with 3-triethoxysilyl propylamine (APTES) or impregnated with polyethyleneimine (PEI). CO_2 isotherms were measured and well described by the Dual site Langmuir model for all adsorbents and CO_2 uptakes were correlated with the different frameworks. It was found that the addition of fluoride is a key factor in the regulation of CO_2 uptake by physisorption and chemisorption.

KEYWORDS: APTES, chemisorption, fluoride, SBA-15.

1. INTRODUCTION.

Global warming resulting from the emission of greenhouse gases has received widespread attention due to the significant and continuous rise in atmospheric CO_2 concentration, mainly by the extensive utilization of fossil fuels. Previous researchers have established that anthropogenic CO_2 accounted for more than 60% of the total emissions leading to global warming (Houghton et al., 1990). Accordingly, considerable efforts have been devoted to develop new technologies to redress the massive CO_2 discharges. Generally, the main approaches to the separation of CO_2 are cryogenic distillation, membrane purification, absorption with liquids and

adsorption using solids (Choi et al., 2009; Douglas et al., 2005). The absorption with liquids is the most mature technology for large-scale CO_2 capture using aqueous alkylamine solutions or other fluids with basic character, such as chilled ammonia, which chemically absorbs the acid gases (Danckwerts, 1979; Astarita, 1961) However, the alkylamine solutions have some drawbacks such as high equipment corrosion rate due to evaporation process, high energy consumption in regeneration, loss of effectiveness over time due to low thermal stability and high footprint requirements (Rinker et al., 2000). An alternative technique to the sequestration of CO_2 is the adsorption over porous adsorbents functionalized with organic molecules containing amino groups due to its low energy requirement and easy operation and maintenance. In addition, the adsorption process exhibits several advantages over liquid amines such as a minor solvent loss that reduces the vessel corrosion and the regeneration process is easier (Sayari et al., 2011) Nevertheless, CO_2 adsorption in such materials is still far from the requirements of industrial practice so the optimization of the synthesis is a challenge for the researchers.

Several solid adsorbents may be suited for amine grafting, such as SBA-15 silicas (Wang and Yang, 2011) and mesocelular silica foams (Heydary-Gorji et al., 2011). These have received considerable research interest due to their high adsorption capacity, storage and selectivity towards CO_2, SBA-15 being the most studied porous silica due to the larger pore size (5-30 nm) as well as a high wall thickness, which ensures its thermal, mechanical and chemical resistance in comparison with other hexagonal mesoporous silicas, as MCM-41.

2. EXPERIMENTAL.

2.1. Preparation of Siliceous Porous Structures.

Traditional SBA-15 was synthesized based on the method reported by Fulvio et al. (2005). Briefly, pluronic (P123) was firstly dissolved in 1.7 M HCl (aq.) at 313 K and then TEOS was added dropwise. The final molar composition of the synthesis gel was $P123/SiO_2/HCl/H_2O$ = 0.018/1/6.364/202. The resulting suspension was stirred at 313 K for 24 h and then transferred to a Teflon-lined autoclave, where it was hydrothermally treated at 393 K for 72 h. The solid was then filtered, washed with deionized water and dried at 333 K overnight (S00).

Mesocellular silica foams (MCFs) were prepared according to the water-alkane emulsion method proposed by Bao and co-workers (2006). In a first step, P123 and different amounts of NH_4F were dissolved in 1.7 M HCl (aq.) at 313K for 24 h, and then TEOS was premixed with heptane and added into the transparent solution with further stirring for 24 h at room temperature. The final molar ratios in the synthesis gel were set to $P123/SiO_2/HCl/NH_4F/heptane/H_2O$ = 0.018/1/ 6.364/0-0.065/4.273/202. The resulting white suspension was then transferred to a Teflon-lined autoclave and hydrothermally treated at 393 K for 72 h. The solid was finally filtered, washed with deionized water and dried overnight at 333 K.

All materials were calcined from room temperature to 550 ºC at a heating rate of 1 ºC min^1 and maintained at this temperature for 6 h. The mesostructured materials were denoted as S00 for the traditional SBA-15 and S1*x* ("1" for materials with heptane) where *x* increases from 1 to 4, standing for the F/Si molar ratio.

2.2. Grafting of 3-(triethoxysilyl) propylamine (APTES) and impregnation of poly (ethyleneimine) (PEI).

The grafting of APTES in each support was carried out by following the methodology reported by Hiyoshi et al. (2004). The impregnation via incipient wetness of siliceous porous materials was performed with PEI in methanol (Xu et al., 2003).

2.3. Characterization techniques.

The samples were characterized by N_2 adsorption/desorption isotherms, transmission electron microscopy (TEM), X-ray diffraction; FT-IR spectroscopy and elemental chemical analysis.

2.4. CO_2 adsorption tests

CO_2 adsorption isotherms were measured with a Micromeritics ASAP 2020 Analyzer (i.e., volumetrically) at 25 ºC. Constant temperature circulating baths were used to maintain the sample at 25 ºC. Prior to the measurements, samples were outgassed at 115 ºC and 10^{-4} mbar overnight

3. RESULTS AND DISCUSSION.

3.1. Materials characterization: Small-angle X-ray patterns of the synthesized porous silicas are shown in Figure 1. Conventional hydrothermal SBA-15 (S00) shows a typical XRD pattern of an ordered hexagonal network of mesopores with (100), (110) and (200) plane reflections that suggest a long-range order, characterizing a well-ordered mesoporous structure with P6mm hexagonal symmetry (Zhao et al., 1998) in some of the studied samples. TEM micrograph reveals a well-ordered honeycomb structure which agrees with the findings from the small-angle XRD diffractogram.

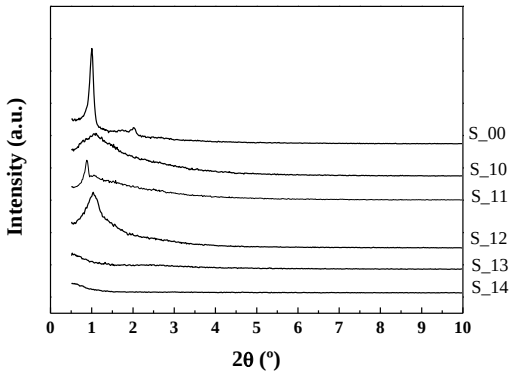

Figure 1. XRD patterns of pure SBA-15 (S00), SBA-15 with heptane (S10) and with heptane and rising the amount of fluoride (S11, S12,S13 and S14).

The addition of the swelling agent during the synthetic process, such as heptane, leads a poor resolution of the (100) diffraction peak and the absence of the (110) and (200) reflections, which suggests that pore swelling agents like heptane attach to the surface functional groups giving rise to less ordered materials. This disordering effect was confirmed by TEM micrographs (Figure 2).

With this respect, other authors (Schmidt-Winkel et al., 2000) have established that the transition from the hexagonally structured SBA-15 and a mesocellular foam takes place due to an increase in the pore size caused by such swelling agents as alkanes or benzene derivatives compounds, which penetrate into the hydrophobic core of the surfactant micelle, disrupting the typical honey comb packing of the hydrothermal SBA-15 by leading the nodes to separate into spherical micelles and aggregate to form the mesocellular foam material, as revealed by the TEM micrographs.

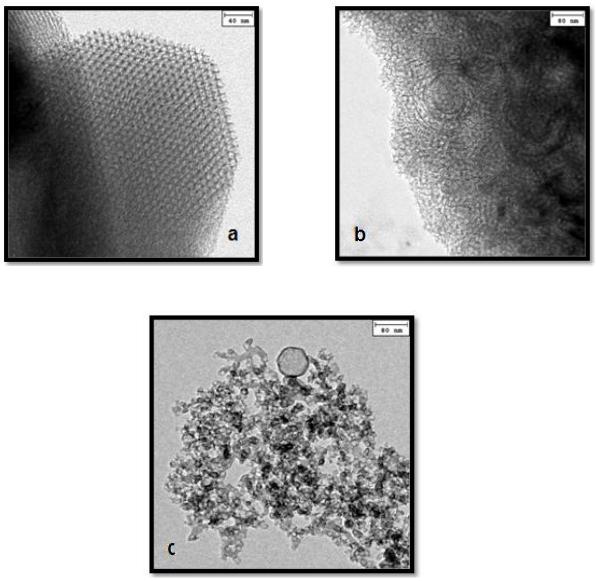

Figure 2. TEM micrographs of (a) SBA-15 (S00), (b) SBA-15 with heptane (S10) and (c) with the highest fluoride load (S14) and heptane.

In figure 3, N_2 adsorption/desorption isotherms are shown for samples S00, S10 and S14. The addition of ammonium fluoride produces a shift of the hysteresis loop to higher relative pressure. Low loads of ammonium fluoride lead to a significant decrease in the surface area (Table 1). Nevertheless, for higher fluoride content, the surface area and nitrogen adsorbed at higher relative pressure increase with narrow hysteresis loop, which indicates the formation of a uniform structure with larger pore size. Textural properties (see Table 1.) suggests a progressive loss of the ordered framework leading to a structure with low porosity that evolves to MCF structure when the fluoride content is increased, in according with DRX patterns.

Table 1. Textural properties of pure mesoporous silicas

	S (m^2/g)	D_p (nm)	V_p (cm^3/g)	V_{mpDR} (cm^3/g)
S00	908	7.95	1.70	0.45
S10	643	10.7	1.84	0.32
S11	392	16.6	1.03	0.24
S12	542	13.5	1.71	0.28
S13	418	15.3	1.68	0.15
S14	447	17.3	2.33	0.23

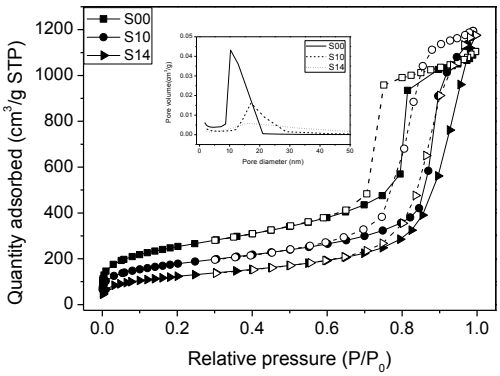

Figure 3. Nitrogen adsorption/desorption isotherms at -196ºC for pure supports S00, S10 and S14.

The vibration frequencies and their respective roles in the porous silica framework were examined by FT-IR spectroscopy in the range of 4000-400 cm^{-1}. The FT-IR spectra for all samples are typically dominated by the Si–O–Si asymmetric stretching at 1054 cm^{-1} with a shoulder at 1160 cm^{-1}, revealing the existence of a dense silica network, where oxygen atoms play the role of bridges between two silicon sites. The symmetric vibration at 805 cm^{-1} was assigned to the Si–O–Si bending mode. The band at 960 cm^{-1} can be assigned to the Si–O in-plane stretching vibrations of the silanol Si-OH groups generated by the presence of defect sites (Colilla et al., 2010). The bands in the range of 3740-3415 cm^{-1} were assigned to the overlapping of the O-H stretching bands of hydrogen-bonded water molecules (H-O-H) and Si-OH stretching mode of surface silanol hydrogen bonded to molecular water ($SiOH\cdots H_2O$) (Gallas and Lavelley, 1990). Finally, the band located at 1631 cm^{-1} has been assigned to H-O-H bending vibrations (Colilla et al., 2010).

The functionalization of silica porous materials with organic molecules containing amino groups reveals the presence of two bands located at 2950 and 2840 cm^{-1} assigned to C-H asymmetric stretching and symmetric stretching modes of PEI (Figure 3) and APTES chains (Drage et al., 2008). The bands centered between 1565 and 1485 cm^{-1} are assigned to asymmetric and symmetric bending of primary amines ($-NH_2$) (Wang et al., 2009). Nonetheless, the band located at 1485 cm^{-1} can also be ascribed to the deformation of C-H bond (Lakard et al., 2004). The band located at 1310 cm^{-1} has been assigned to NCOO- skeletal vibration (Wang et al., 2009). Moreover, in the case of the grafted porous silica, the presence of two bands located at 3364 and 3289 cm^{-1}, assigned to N-H stretching vibration, is noticeable (Wang et al., 2009) and so is the presence of a band located at about 687 cm^{-1}. It has been ascribed to the presence of N-H bending vibrations, indicating that the amine group in APTES-functionalized SBA-15 material has been successfully obtained (Han et al., 2007). Finally, the intensity of the band corresponding to silanol groups (960 cm^{-1}) decreases and/or is not observed in the FT-IR spectra of the functionalized porous silicas, suggesting a possible reaction between the silanol group from the silica surface and the amine group of PEI or APTES, giving evidence to the covalent bonding of organic molecules containing the amino group in porous silica materials.

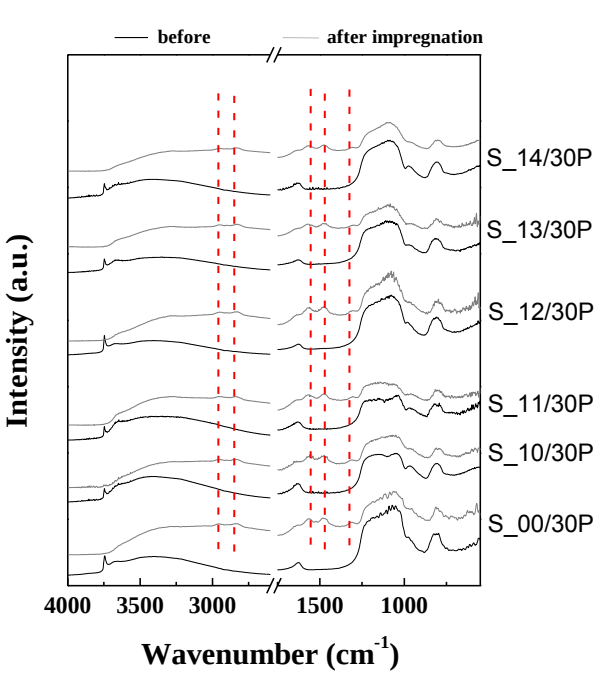

Figure 4. FTIR spectra of the pure supports (Black line) and after impregnation with 30% PEI (grey line)

3.1. CO_2 adsorption isotherms Some selected CO_2 isotherms at 25ºC for the grafted and impregnated series are shown in Figs. 5 and 6, respectively. The structure of all adsorbents and the chemistry of amino sources have an important influence in CO_2 uptakes. In fact, the measured experimental data were well fitted by Dualsite Langmuir model (Equation 1).

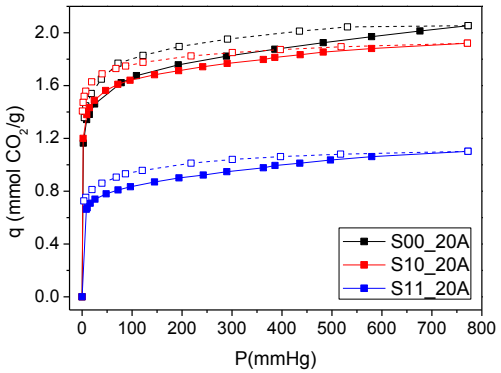

Figure 5. CO_2 isotherms at 25ºC on grafted silicas S00, S10 and S11 with 20%APTES.

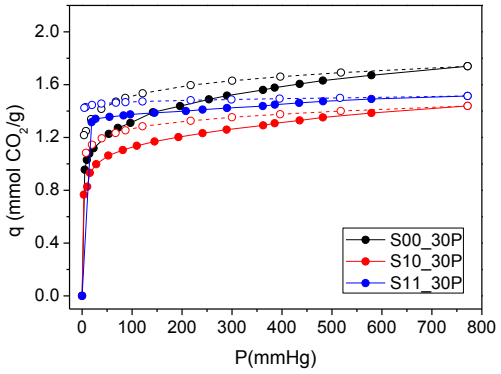

Figure 6. CO_2 isotherms at 25ºC on impregnated silicas S00, S10 and S11 with 30% PEI.

$$Q = \frac{Q_{max1} * K_1 * P}{1 + K_1 * P} + \frac{Q_{max2} * K_2 * P}{1 + K_2 * P}$$ **Equation 1**

With this model, we have assumed (Vilarrasa-Garcia et al., 2014) that there are two different adsorption sites which are related to chemisorption (depends to amino groups, q_{m1}) and physisorption (related to siliceous framework, site 2, q_{m2}). Tables 2 and 3 summarize DL model parameters for APTES-grafted and PEI-impregnated supports, respectively. CO_2/N ratio and % N (wt) as determined by elemental analysis are also showed.

If only the adsorbents prepared with fluoride were considered, it can be observed that the increase in the amount of fluoride promotes an increase in the physical affinity as reflected in the larger K_2 obtained. However, the less ordered structure of these solids impedes the presence of two adjacent amino groups when APTES is grafted, which are required to react thus the addition of fluoride provokes a decrease in the availability of chemisorption sites.

In the case of the adsorbents impregnated with PEI, it can be observed that the ratio $q_{chemisorption}/q_{total}$ increases with the addition of fluoride. The presence of PEI blocks micropores, which leads to a decrease in physisorbed CO_2, especially in the samples with a larger microporosity. Although the PEI-impregnated adsorbents have inaccessible amino groups below 75ºC, CO_2 capacities obtained at 25ºC are noticeable. On the other hand, the maximum value reached at 1 bar and 25ºC is 2.3 mmol CO_2/g (253 mg/g PEI) at a PEI load to 40%.

With the Dualsite model parameters, the contribution of physisorption and chemisorption were plotted as separate isotherms for all samples (see Figs. 7-10), corresponding to each of the two terms of the summation of the DL model. In these figures, it can be observed that S11 sample has the lowest physisorption capacity and when it is impregnated with PEI, it reaches the highest CO_2 capacity by chemisorption. With the addition of a low amount of fluoride (S11), 90% of highest chemisorption capacity is achieved.

Table 2. DL model parameters and N content (%wt) obtained by chemical elemental analysis for grafted silicas

20 APTES	Q (mmol CO_2/g)	DualSite Langmuir					%N	mol CO_2/mol N chemisorption	% q_{m1}/q_t
		Q_{max1}	K_1	Q_{max2}	K_2	Chi2			
S14	1.33	0.88	0.595	0.73	2.3E-3	3.2E-4	3.27	0.37	65.45
S13	1.37	0.96	0.689	0.71	1.9E-3	8.6E-6	5.48	0.41	69.75
S12	1.18	0.73	0.364	0.78	1.8E-3	1.6E-5	3.03	0.34	61.52
S11	1.11	0.76	0.674	0.65	1.5E-3	1.5E-5	2.86	0.37	68.72
S10	1.92	1.46	1.759	0.57	4.3E-3	2.1E-4	5.68	0.36	76.09
S00	2.12	1.44	1.428	0.91	2.6E-3	7.3E-4	4.97	0.41	67.94

Table 3. DL model parameters and N content (%wt) obtained by chemical elemental analysis for impregnated silicas

30 PEI	Q (mmol CO_2/g)	DualSite Langmur					%N	mol CO_2/mol N chemisorption	% q_{m1}/q_t
		Q_{max1}	K_1	Q_{max2}	K_2	Chi2			
S14	1.49(218)[a]	1.14	1.358	0.46	3.7E-3	8.2E-5	8.43	0.19	76.44
S13	1.34(196)[a]	1.11	2.589	0.35	2.5E-3	5.7E-5	7.21	0.19	82.41
S12	1.35(198)[a]	1.02	0.652	0.75	1.0E-3	2.3E-5	7.95	0.14	75.54
S11	1.51(221)[a]	1.35	1.933	0.61	5.0E-4	2.2E-5	10.24	0.24	89.19
S10	1.44(211)[a]	0.97	0.813	0.63	3.0E-3	4.9E-4	8.37	0.19	67.58
S00	1.74(255)[a]	1.13	0.891	0.86	2.9E-3	8.2E-5	8.53	0.19	64.72

[a]CO_2 capacity in mg CO_2/g PEI

.

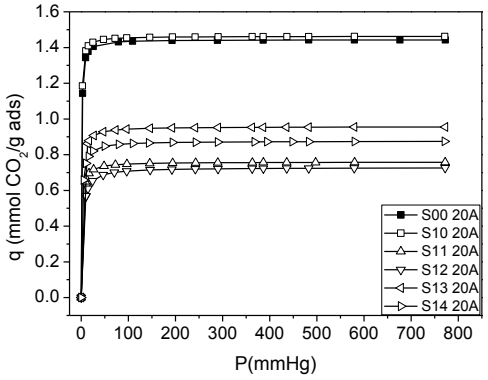

Figure 7. CO_2 chemisorption isotherms at 25ºC obtained from DL model for all grafted sílicas.

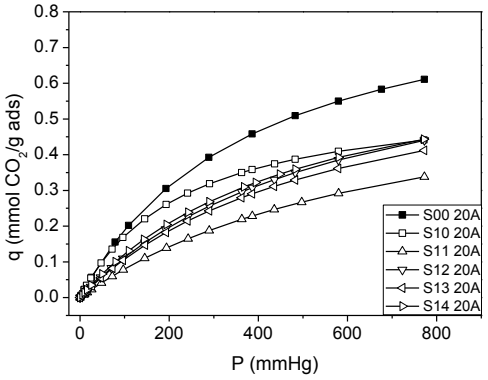

Figure 8. CO_2 physisorption isotherms at 25ºC obtained from DL model for all grafted sílicas.

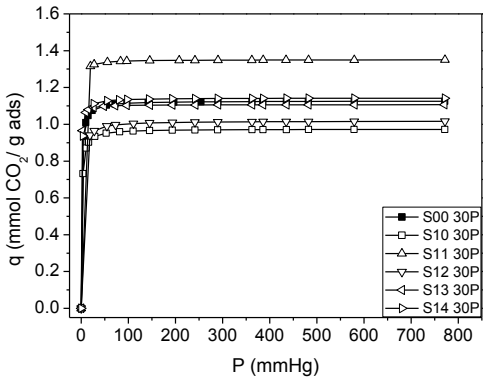

Figure 9. CO_2 chemisorption isotherms at 25ºC obtained from DL model for all impregnated sílicas.

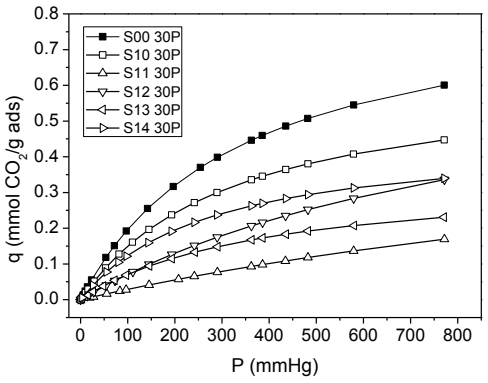

Figure 10. CO_2 physisorption isotherms at 25ºC obtained from DL model for all impregnated sílicas.

4. CONCLUSIONS

Several mesoporous silicas with a less ordered hexagonal structure have been synthesized. The evolution to less ordered materials was achieved by the addition of a swelling agent and modifying with the addition of different amounts of fluoride. The supports were loaded with amino groups by using two different strategies: PEI impregnation and APTES grafting. PEI and APTES, as amino sources, were effectively incorporated on the surface of materials, as confirmed by chemical elemental analysis and FTIR. Adsorbents who have a less ordered structure exhibit a better ratio chemisorption/physisorption and potentially these materials are interesting CO_2 adsorbents when the temperature is increased. The addition of low amounts the fluoride leads to hybrid material between honeycomb and MFC structure, decreases micropore volume and enhances the chemisorption ratio as it was reported in previous studies (Vilarrasa-Garcia et al., 2014).

5. ACKNOWLEDGMENTS

The authors acknowledge financial support provided by the Spanish Ministry of Economy and Competitiveness CTQ2012-37925-C03 and FEDER funds, the Regional Government (Junta de Andalucia) P09-FQM-5070, the European Union Grant 295156, FP7-PEOPLE-2011-IRSES and Brazil-Spain Project PHB2011-0074-PC.

6. REFERENCES

ASTARITA, G., *Chem. Eng. Sci*. v. 16, p.202-207, 1961.

CHOI, S., DRESE, J.H., JONES, C.W. *ChemSusChem*. v. 2, p. 796-854, 2009.

COLILLA, M., IZQUIERDO-BARBA, I., SÁNCHEZ-SALCEDO, S., FIERRO, J.L.G, HUESO, J.L., VALLET-REGÍ, M. *Chem. Mater*. v.22, p. 6459-6460, 2010.

DANCKWERTS, P. V. *Chem. Eng. Sci*. v. 34, p. 443-446, 1979.

DOUGLAS, A., COSTAS, T. *Sep. Sci. Technol*. v.40, p. 321-348, 2005).

DRAGE, T.C., ARENILLAS, A., SMITH, K.M., SNAPE, C.E. *Micropor. Mesopor. Mater*. v..116, p. 504-512, 2008.

FULVIO, P.F., PIKUS, S., JARONIEC, M.J. *Mater. Chem*. v.15, p. 5049-5053, 2005.

GALLAS, J.P., LAVELLEY, J.C. *Langmuir*.v. 6, p.1364-1372, 1990.

HAN, L., RUAN, J.F., LI, Y.S., TERASAKI, O., CHE, S.A. *Chem. Mater*., v. 19, p. 2860-2867, 2007.

HEYDARI-GORJI, A., YANG, Y., SAYARI, A. *Energy & Fuels*. v. 25, p. 4206-4210, 2011.

HIYOSHI, N., YOGO, K., YASHIMA, T., *Stud. Surf .Sci. and Catalysis.*, v. 154, p. 2995-3002, 2004.

HOUGHTON, J.T., JENKINS, G.J., EPHRAUMS, J.J. (Eds.), IPCC First Assessment Report 1990 (FAR) Intergovernmental Panel on Climate Change (IPCC), Cambridge Univ. Press, New York, 1990.

LAKARD, S., HERLEM, G., LAKARD, B., FAHYS, B. *J. Mol. Struct-Theochem*.. v. 685, p. 83-87, 2004.

RINKER, E., ASHOUR, S.S., SANDALL,O.C. *Ind. Eng. Chem. Res*. v. 39, p. 4346-4356., 2000).

SAYARI, A., BELMABKHOUT, Y., SERNA-GUERRERO, R. *Chem. Eng. J*. v. 171, p. 760–774, 2011.

SCHMIDT-WINKEL, P., LUKENS JR. , W.W., YANG, P., MARGOLESE, D.I., LETTOW, J.S., YING, J.Y., STUCKY, G.D., *Chem. Mater*, v. 12, p. 686-696, 2000.

VILARRASA-GARCÍA, E., CECILIA, J.A., SANTOS, S.M.L., CAVALCANTE JR., C.L., JIMENEZ-JIMENEZ, J.L., AZEVEDO, D.C.S., RODRIGUEZ-CASTELLON, E., *Micropor. Mesopor. Mater.*, v. 187, p. 125-134, 2014.

XU, X., SONG, C., ANDRESEN, J.M., MILLER, B.G.,SCARONI, A. W. *Micropor. Mesopor. Mater.*, v. 62, p. 29-45, 2003.

ZHANG, H., SUN, J., MA, D.,WEINBERG, G., SU, D.S., BAO, X. *J. Phys. Chem. B.*v. 110, p.25908-25915, 2006.

ZHAO, D., FENG, J., HUO, Q., MELOSH, N., FREDRICKSON, G.H., CHMELKA, B.F, STUCKY, G.D. *Science*. v.279, p. 548-552, 1998.